

STRESS INTENSITY FACTORS FOR SURFACE AND CORNER CRACKS
EMANATING FROM A WEDGE-LOADED HOLE¹

113082

W. Zhao and M.A. Sutton
University of South Carolina
Columbia, SC 29208

K.N. Shivakumar
North Carolina A & T State University
Greensboro, NC 27410

J.C. Newman, Jr.
NASA Langley Research Center
Hampton, VA 23681-0001

ABSTRACT

To assist analysis of riveted lap joints, stress intensity factors are determined for surface and corner cracks emanating from a wedge-loaded hole by using a 3-D weight function method in conjunction with a 3-D finite element method. A stress intensity factor equation for surface cracks is also developed to provide a closed-form solution. The equation covers commonly-encountered geometrical ranges and retains high accuracy over the entire range.

INTRODUCTION

Current damage tolerance analysis of aircraft structures is mainly based on linear elastic fracture mechanics, where the stress intensity factor is a key parameter. Surface and corner cracks emanating from circular holes are among the most common defects occurring in aircraft structures. Stress intensity factor solutions for these cracks are available in the literature for remote tension and remote bending [1-5]. Based on three-dimensional finite element solutions, the corresponding stress intensity factor equations were also developed [3], and are being used in a variety of applications. However,

¹ Work done on contract at University of South Carolina, NAG-1-1489.

for another important category of loading conditions (i.e. wedge loading of a cracked hole) very limited solutions [1,4] exist in the literature for corner cracks, and no solution is available for surface cracks. The primary interest in the wedge loading case lies in the fact that solutions for commonly encountered pin-loading case, such as the riveted lap joints shown in Fig.1, can be obtained by superposing solutions for remote tension, remote bending and wedge loading. The objective of this paper is to provide stress intensity factor solutions for surface and corner cracks emanating from a wedge-loaded hole, which can be used to obtain solutions for rivet loading. This is accomplished in two ways. First, an accurate and efficient 3-D weight function method [5] is extended to solve the problems by using stress distributions from a 3-D finite element analysis of the same, but otherwise uncracked, configuration. The weight-function analysis code covers a wide range of geometrical parameters and various loading conditions, and produces accurate solutions on Personal Computers. Second, a stress intensity factor equation for surface cracks is developed by curve-fitting procedures. This latter effort is to facilitate the determination of stress intensity factors for commonly-encountered surface cracks in damage tolerance analysis.

METHODS OF ANALYSIS

The crack configurations to be considered are shown in Fig.2 together with the definition of relevant parameters (infinite plate width and height assumed). The 3-D weight function method is used in combination with the 3-D finite element method to solve these problems. This combined approach takes optimal advantage of both methods. The weight function method is accurate and efficient in solving 3-D crack configurations. However, its accuracy can not be guaranteed without using, as input, an accurate stress solution for the same, but otherwise uncracked, configuration. For crack configurations involving stress concentrations (such as a hole or notch), the stress distribution in the region of uncracked configuration where cracks will occur has a fully 3-D nature, the stress varies not only in plate-width direction but also in thickness directions, even though the applied load does not change through the plate thickness. This 3-D effect manifests itself most near the intersection of the hole with the plate surface for small r/t ratios (see for example [6,7]). Therefore, to account for this 3-D nature, a 3-D finite element analysis was performed [7] to provide the normal stress distributions. Because the finite element analysis involves no cracks, only one finite element calculation is required for each r/t ratio. The normal stress distribution obtained from the finite element analysis is then fitted into the following equation:

$$\sigma(x,y)/\sigma_0 = \sum_{i=1}^I \sum_{j=1}^J C_{ij} \left(\frac{x}{r}\right)^{2-2i} \left(\frac{y}{t}\right)^{2j-2} \quad (1)$$

Equation (1) is used in the following weight function equations:

$$K_a(x, a_x) = \int_0^{a_x} [\sigma(x, y) - P(x, y)] W_a(a_x, y) dy \quad (2a)$$

$$K_c(y, c_y) = \int_0^{c_y} P(x, y) W_c(c_y, x) dx \quad (2b)$$

where $K_a(x, a_x)$ and $K_c(y, c_y)$ are, respectively, stress intensity factors for a-slice and c-slice, intersecting at point (x, y) on the crack front (see Fig. 2 (d) and (e)), and W_a and W_c are the weight functions. The stress intensity factors for the 3-D crack, $K(\varphi)$, are then obtained by eq.(3):

$$K(\varphi) = \frac{(-1)^n}{1 - \eta^2(\nu, a/c, \Delta\varphi)} \left\{ K_a^4(x, a_x) + \left[\frac{E}{E_s} K_c(y, c_y) \right]^4 \right\}^{\frac{1}{4}} \quad (3)$$

For further details of the weight function method, please refer to [5].

RESULTS AND COMPARISONS

The stress intensity factors are presented in a dimensionless form defined as:

$$F(\varphi) = K(\varphi) / (\sigma \sqrt{\pi a / Q}) \quad (4)$$

in which σ is a reference stress, and equal to remote uniform stress for remote tension, and $\sigma = P / (2rT)$ for wedge loading, where P is the total applied force along the bore of the hole.

Corner Cracks

Reference [1] provides stress intensity factors for wedge loading with a cosine squared pressure distribution, while the present weight function solutions are for wedge loading with a cosine pressure distribution. However, the difference caused by the different pressure distributions will be negligible, as long as the c/r ratio of cracks exceeds about 0.8. The following comparisons are made for such cases. Figure 3 shows the comparison of the weight function results with the finite element solution [1]. Very good agreement is observed. Figure 4 (a) shows the difference between a single corner crack and double corner cracks. Figure 4 (b) gives the stress intensity factor ratio of double corner

cracks over single corner cracks. The corresponding estimate by using Shah's empirical formula [8] and the ratios for through-the-thickness cracks [9] are also shown in Fig. 4 (b).

Surface Cracks

The comparison with finite element solution [3] for surface cracks is made for remote tension, since no solution is available for surface cracks under wedge loading in the literature. Figure 5 shows the comparison. Again, very good agreement is observed. To examine the behavior of the weight function method, some limiting cases are also considered as $a/c \rightarrow 0$ and ∞ . Figures 6 (a) and (b) show these limiting cases. It is clear that the appropriate 2-D limits are reached under the limiting conditions.

STRESS INTENSITY FACTOR EQUATION FOR SURFACE CRACKS

In many situations, a closed-form solution is desirable, as evidenced by the popularity of the previous stress intensity factor equations for other cases [3]. Therefore, an effort is made to develop an equation for double surface cracks under wedge loading based on the weight function solutions. The applicable range of the equation is chosen to be $1 \leq r/t \leq 5$, $0.5 \leq a/c \leq 2$ and $0.005 \leq a/t \leq 0.9$. This range is believed to cover most cases encountered in practice. If a problem does go beyond this range, then the weight function code is directly used. The equation is developed separately at 0° and 90° only, so as to reduce the number of independent variables from 4 to 3 (r/t , a/c and a/t). The general form of the equation is:

$$K(\varphi) = \sigma \sqrt{\pi a / Q} F(\varphi) \quad \varphi = 0^\circ, 90^\circ \quad (5)$$

The developments for $F(90^\circ)$ and $F(0^\circ)$ are described in the following sections.

Development of $F(90^\circ)$

The form of $F(90^\circ)$ is:

$$F(90^\circ) = \left(\frac{a}{c}\right)^\gamma f_9\left(\frac{r}{t}, \frac{a}{c}, \frac{a}{t}\right) \quad (6)$$

where $\gamma=0$ for $a/c \leq 1$, and $\gamma=-1$ for $a/c > 1$. The f_9 function is given below:

$$f_9\left(\frac{r}{t}, \frac{a}{c}, \frac{a}{t}\right) = g_9\left(\frac{r}{t}, \frac{a}{c}, \frac{a}{t}\right) f_{sa}\left(\frac{x}{r}, \frac{a}{t}\right) \quad (7)$$

where g_9 is a fitting function, and f_{sa} is a combination of the two functions $f_s(x/r)$ and $f_a(a/t)$. The $f_s(x/r)$ is the dimensionless normal stress distribution along the x-axis for a wedge loaded hole in an infinite plate. According to Rooke & Tweed [10], $f_s(x/r)$ is expressed as:

$$f_s\left(\frac{x}{r}\right) = \frac{\sigma(x)}{\sigma} = \frac{4}{\pi} \left\{ 3 + \frac{1}{\left(1 + \frac{x}{r}\right)^2} + \frac{1 + 2\left(1 + \frac{x}{r}\right)^2 - 3\left(1 + \frac{x}{r}\right)^4}{2\left(1 + \frac{x}{r}\right)^3} \ln \left[\frac{2 + \frac{x}{r}}{\frac{x}{r}} \right] \right\} \quad (8)$$

The $f_a(a/t)$ is the dimensionless stress intensity factor for collinear cracks, and given as [11]:

$$f_a\left(\frac{a}{t}\right) = \left[\tan\left(\frac{\pi a}{2t}\right) / \left(\frac{\pi a}{2t}\right) \right]^{\frac{1}{2}} \quad (9)$$

The introduction of f_s and f_a is based on the consideration that $F(90^\circ) = f_s(0) * f_a(a/t)$ as $a/c \rightarrow 0$. Using f_s and f_a , f_{sa} is defined as:

$$f_{sa}\left(\frac{c}{r}, \frac{a}{t}\right) = \frac{1}{4} \left[3f_s(0)f_a\left(\frac{a}{t}\right) + f_s\left(\frac{c}{r}\right)f_a(0) \right] \quad (10)$$

The use of f_{sa} is to bring in some of the contributions of the rest of the crack to $F(90^\circ)$. The use of these functions is believed to be very helpful in fitting complicated functions involving multiple variables in a wide range. The g_9 is fitted in the following form:

$$g_9\left(\frac{r}{t}, \frac{a}{c}, \frac{a}{t}\right) = \alpha_1\left(\frac{r}{t}, \frac{a}{t}\right) * \left(\frac{a}{c}\right)^{\alpha_2\left(\frac{r}{t}, \frac{a}{t}\right)} \quad (11)$$

The functions $\alpha_1(r/t, a/t)$ and $\alpha_2(r/t, a/t)$ are expressed as:

$$\alpha_1\left(\frac{r}{t}, \frac{a}{t}\right) = \left\{ \alpha_{11}\left(\frac{r}{t}\right) + \alpha_{12}\left(\frac{r}{t}\right) * \left(\frac{a}{t}\right)^3 \right\} * \exp\left[\alpha_{13}\left(\frac{r}{t}\right) * \left(\frac{a}{t}\right) \right]$$

$$\alpha_{11}\left(\frac{r}{t}\right) = \alpha_{111} * \left(\frac{r}{t}\right)^{\alpha_{112}}$$

$$\alpha_{12}\left(\frac{r}{t}\right) = \alpha_{121} + \alpha_{122} * \left(\frac{r}{t}\right)$$

$$\alpha_{13}\left(\frac{r}{t}\right) = \alpha_{131} + \alpha_{132} * \left(\frac{r}{t}\right) + \alpha_{133} \left(\frac{r}{t}\right)^2$$

$$\alpha_2\left(\frac{r}{t}, \frac{a}{t}\right) = \left\{ \alpha_{21}\left(\frac{r}{t}\right) + \alpha_{22}\left(\frac{r}{t}\right) * \left(\frac{a}{t}\right) + \alpha_{23}\left(\frac{r}{t}\right) * \left(\frac{a}{t}\right)^2 \right\} * \cos\left[\alpha_{24}\left(\frac{r}{t}\right) * \left(\frac{a}{t}\right)^3 \right]$$

$$\alpha_{2i}\left(\frac{r}{t}\right) = \alpha_{2i1} + \alpha_{2i2} * \left(\frac{r}{t}\right) + \alpha_{2i3} * \left(\frac{r}{t}\right)^2 + \alpha_{2i4} * \left(\frac{r}{t}\right)^3, \quad i=1,2,3,4.$$

The α parameters with 3-digit subscripts are constants, and listed in Table 1.

Development of $F(0^\circ)$

The functional form of $F(0^\circ)$ is given as:

$$F(0^\circ) = \left(\frac{a}{c}\right)^\lambda f_0\left(\frac{r}{t}, \frac{a}{c}, \frac{a}{t}\right) \quad (14)$$

where $\lambda=1/2$ for $a/c \leq 1$, and $\lambda=-1/2$ for $a/c > 1$. The f_0 function is given below:

$$f_0\left(\frac{r}{t}, \frac{a}{c}, \frac{a}{t}\right) = g_0\left(\frac{r}{t}, \frac{a}{c}, \frac{a}{t}\right) f_c\left(\frac{c}{r}\right) t_0\left(\frac{r}{t}, \frac{a}{c}, \frac{a}{t}\right) \quad (15)$$

where g_0 and t_0 are fitting functions, and f_c is a weighted average of $f_{c0}(c/r)$. The latter is the dimensionless stress intensity factor for through-the-thickness cracks under the same loading, and given as:

$$f_{c0}\left(\frac{c}{r}\right) = 1.788 - 4.935\left(\frac{c}{r}\right) + 8.527\left(\frac{c}{r}\right)^2 - 7.790\left(\frac{c}{r}\right)^3 + 3.450\left(\frac{c}{r}\right)^4 - 0.5832\left(\frac{c}{r}\right)^5 \quad (16)$$

Then, f_c is defined as:

$$f_c\left(\frac{c}{r}\right) = \frac{1}{4} \left[3f_{c0}\left(\frac{c}{r}\right) + f_{c0}(0) \right] \quad (17)$$

Similarly to $F(90^\circ)$, the introduction of f_{c0} is based on the consideration that $F(0^\circ) = f_{c0}(c/r)$ as $a/c \rightarrow \infty$. And f_c is used to bring in some of the contributions of the rest of the crack to $F(0^\circ)$. The g_0 is fitted in the following form:

$$g_0\left(\frac{r}{t}, \frac{a}{c}, \frac{a}{t}\right) = \beta_1\left(\frac{r}{t}, \frac{a}{t}\right) * \left(\frac{a}{c}\right)^{\beta_2\left(\frac{r}{t}, \frac{a}{t}\right)} \quad (18)$$

The functions $\beta_1(r/t, a/t)$ and $\beta_2(r/t, a/t)$ are expressed as:

$$\begin{aligned} \beta_1\left(\frac{r}{t}, \frac{a}{t}\right) &= \beta_{11}\left(\frac{r}{t}\right) * \text{Exp} \left[\beta_{12}\left(\frac{r}{t}\right) * \left(\frac{a}{t}\right) + \beta_{13}\left(\frac{r}{t}\right) * \left(\frac{a}{t}\right)^3 \right] \\ \beta_{11}\left(\frac{r}{t}\right) &= \beta_{111} + \beta_{112} * \left(\frac{r}{t}\right) \\ \beta_{12}\left(\frac{r}{t}\right) &= \beta_{121} + \beta_{122} * \left(\frac{r}{t}\right) + \beta_{123} * \left(\frac{r}{t}\right)^2 + \beta_{124} * \left(\frac{r}{t}\right)^3 \\ \beta_{13}\left(\frac{r}{t}\right) &= \beta_{131} + \beta_{132} * \left(\frac{r}{t}\right) + \beta_{133} * \left(\frac{r}{t}\right)^2 \end{aligned} \quad (19)$$

$$\begin{aligned} \beta_2\left(\frac{r}{t}, \frac{a}{t}\right) &= \left\{ \beta_{21}\left(\frac{r}{t}\right) + \beta_{22}\left(\frac{r}{t}\right) * \left(\frac{a}{t}\right)^{\frac{1}{2}} \right\} * \text{Exp} \left\{ \beta_{23}\left(\frac{r}{t}\right) * \left(\frac{a}{t}\right) + \beta_{24}\left(\frac{r}{t}\right) * \left(\frac{a}{t}\right)^2 \right\} \\ \beta_{2i}\left(\frac{r}{t}\right) &= \beta_{2i1} + \beta_{2i2} * \left(\frac{r}{t}\right) + \beta_{2i3} * \left(\frac{r}{t}\right)^2 + \beta_{2i4} * \left(\frac{r}{t}\right)^3, \quad i=1,2,3. \\ \beta_{24}\left(\frac{r}{t}\right) &= \beta_{241} + \beta_{242} * \left(\frac{r}{t}\right) + \beta_{243} * \left(\frac{r}{t}\right)^2 \end{aligned} \quad (20)$$

The β parameters with 3-digit subscripts are constants and listed in Table 2. The t_0 is a fine-tuning function and equal to 1 for $a/t < 0.2$, and fitted as follows for $a/t \geq 0.2$:

$$t_0\left(\frac{r}{t}, \frac{a}{c}, \frac{a}{t}\right) = p_1\left(\frac{r}{t}, \frac{a}{t}\right) + p_2\left(\frac{r}{t}, \frac{a}{t}\right) * \left(\frac{a}{c}\right)^{\frac{1}{4}} + p_3\left(\frac{r}{t}, \frac{a}{t}\right) * \left(\frac{a}{c}\right)^{\frac{1}{2}}$$

$$p_i\left(\frac{r}{t}, \frac{a}{t}\right) = p_{i0}\left(\frac{a}{t}\right) + p_{i1}\left(\frac{a}{t}\right) * \left(\frac{r}{t}\right) + p_{i2}\left(\frac{a}{t}\right) * \left(\frac{r}{t}\right)^2 + p_{i3}\left(\frac{a}{t}\right) * \left(\frac{r}{t}\right)^3 \quad i=1,2,3. \quad (21)$$

$$p_{ij}\left(\frac{a}{t}\right) = p_{j0} + p_{j1} * \left(\frac{a}{t}\right) + p_{j2} * \left(\frac{a}{t}\right)^2 \quad j=0,1,2,3.$$

The constants p_{ijk} for t_0 are given in Table 3.

Comparison of Equation with Weight Function Data

The accuracy of the equation is examined by comparing it with the original weight function data. Figures 7 (a) and (b) give $F(90^\circ)$ and $F(0^\circ)$ versus a/t , respectively. The variations of $F(90^\circ)$ and $F(0^\circ)$ with a/c are shown in Figs. 8 (a) and (b), respectively, which are for $a/t=0.9$, the largest a/t ratio considered. The largest deviation of the equation with the weight function data occurs at this a/t ratio for $F(90^\circ)$. From Fig. 8 (a) the maximum deviation is within 3%. Figures 9 (a) and (b) show $F(90^\circ)$ and $F(0^\circ)$ versus r/t , respectively. It is seen that the equation is generally within 2% of the weight function data, with maximum error of about 3% in the whole range considered.

CONCLUSIONS

Based on the above analysis and results, the following conclusions can be made:

1. The combination of the 3-D weight function method and the 3-D finite element method is an efficient approach to solve 3-D crack problems involving stress concentrations.
2. Accurate stress intensity factors are provided for surface and corner cracks emanating from a wedge-loaded hole.
3. A stress intensity factor equation is developed for double surface cracks. The equation covers commonly-encountered geometrical ranges and retains very good accuracy.

REFERENCES

1. Raju, I.S.; and Newman, J.C., Jr.: Stress intensity factors for two symmetric corner cracks. ASTM STP 677, C.W. Smith, Ed., pp.411-430, 1979.
2. Grandt, A.F., Jr.; and Kullgren, T.E: Stress intensity factors for corner cracked holes under general loading conditions. J. Engng. Materials Technology 103, pp.171-176, 1981.
3. Newman, J.C., Jr.; and Raju, I.S.: Stress intensity factor equations for cracks in three-dimensional finite bodies. ASTM STP 791, Lewis, J.C. and Sines, G., Ed., pp.I-238-256, 1983.
4. Nishioka, T.; and Atluri, S.N.: Integrity analysis of surfaced-flawed aircraft attachment lugs: a new, inexpensive, 3-D alternating method. Paper 82-0742, AIAA/ASME/ASCE/AHS 23rd Structures, Structural Dynamics and Materials Conference, May 10-12, pp.287-300, 1982.
5. Zhao, W.; Wu, X.R.; and Yan, M.G.: Weight function method for three dimensional crack problems-II. Engng. Fracture Mech. Vol.34, No.3, pp.609-624, 1989.
6. Folias, E.S.: Some remarks on three-dimensional fracture. ASTM STP 969, T.A. Cruse, Ed., pp.56-72, 1988.
7. Shivakumar, K.N.; and Newman, J.C. Jr.: Stress concentrations for straight-shank and countersunk holes in plates subjected to tension, bending, and pin loading. NASA-TP-3193, 1992.
8. Shah, R.C.: Stress intensity factors for through and part-through cracks originating at a fastener hole. ASTM STP 590, pp.429-459, 1976.
9. Wu, X.R.; and Carlsson, J.: Weight functions and stress intensity factor solutions. Pergamon press, 1991.
10. Rooke, D.P.; and Tweed, J.: Stress intensity factors for a crack at the edge of a loaded hole. Int. J. Engng. Sci. 18, pp.109-121, 1980.
11. Sneddon, I.N.; and Srivastav, R.P., The stress in the vicinity of an infinite row of collinear cracks, Proc. R. Soc. Edinb., Section A, Vol.67, p.39, 1963-64.

Table 1. Coefficients of g_9 function

	1	2	3	4
α_{11i}	1.292	-0.02280		
α_{12i}	-0.6158	0.03094		
α_{13i}	-0.3834	0.1790	-0.02065	
α_{21i}	0.06285	0.01986	-0.008287	0.0009832
α_{22i}	0.1827	-0.2219	0.08763	-0.01045
α_{23i}	0.09046	-0.02106	-0.02337	0.005125
α_{24i}	1.871	-0.7457	0.4400	-0.05090

Table 2. Coefficients of g_0 function

	1	2	3	4
β_{11i}	0.9708	-0.005293		
β_{12i}	-1.415	0.7752	-0.1815	0.01502
β_{13i}	0.4926	-0.1570	0.01652	
β_{21i}	0.0007527	0.05418	-0.02149	0.002344
β_{22i}	0.4667	-0.4266	0.1586	-0.01709
β_{23i}	3.345	0.04976	-0.6747	0.1018
β_{24i}	-3.626	1.941	-0.2248	

Table 3. Coefficients of t_0 function

	1	2	3
p_{10i}	6.89367	-53.6151	50.8248
p_{11i}	-4.08538	40.9391	-46.3484
p_{12i}	0.677014	-9.35989	12.1718
p_{13i}	-0.0226694	0.668142	-1.00152
p_{20i}	-12.0523	108.472	-102.842
p_{21i}	8.63812	-84.3581	94.9457
p_{22i}	-1.60061	20.0463	-25.5194
p_{23i}	0.0778192	-1.51170	2.15760
p_{30i}	5.83664	-53.1766	50.5411
p_{31i}	-4.20676	41.6555	-46.9805
p_{32i}	0.801768	-10.0724	12.7830
p_{33i}	-0.0421292	0.778241	-1.09613

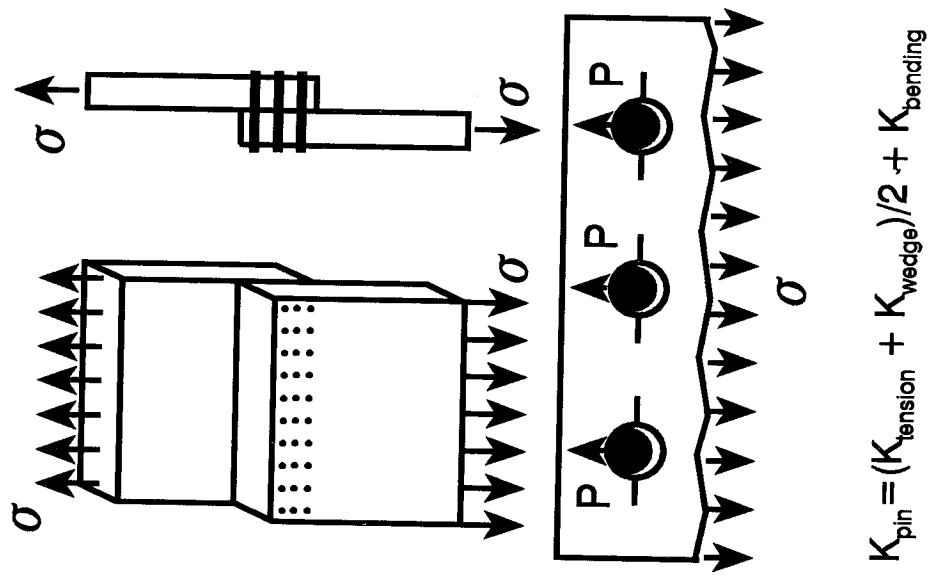


Fig.1 Riveted lap joints with cracks.

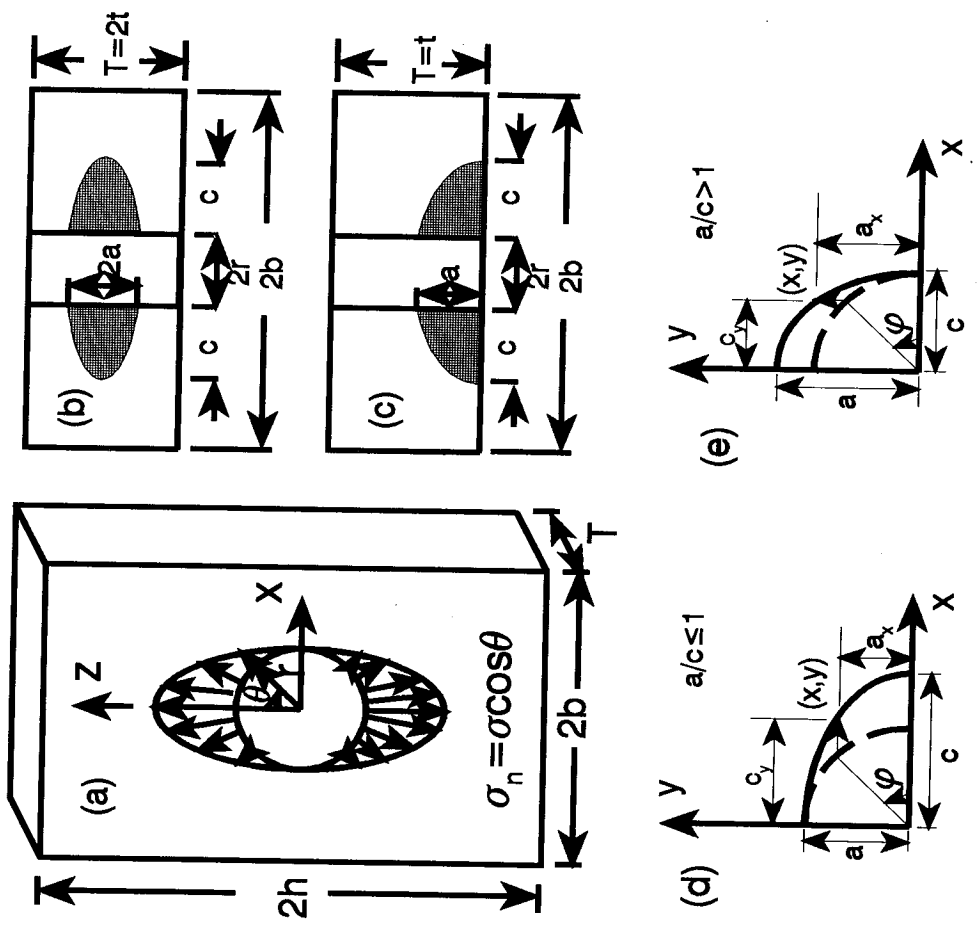


Fig.2 (a) wedge-loaded hole, (b) surface cracks, (c) corner cracks, (d) & (e) crack front coordinates.

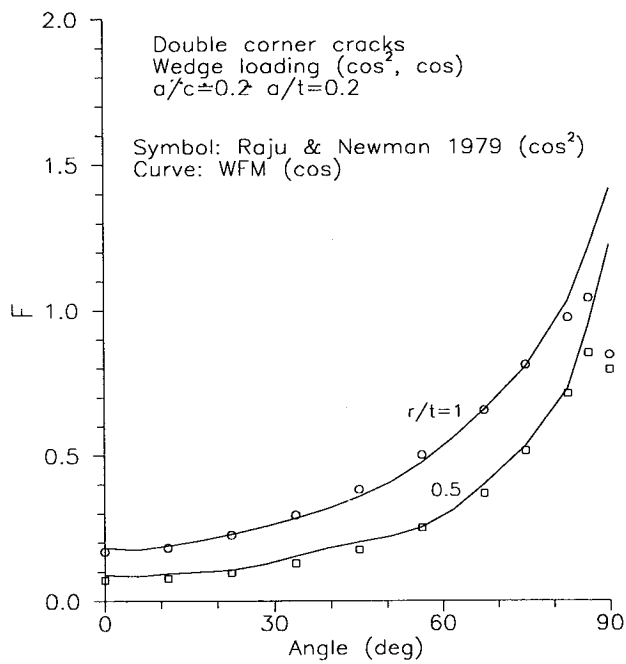


Fig. 3 Comparison of dimensionless stress intensity factors with finite element solutions.

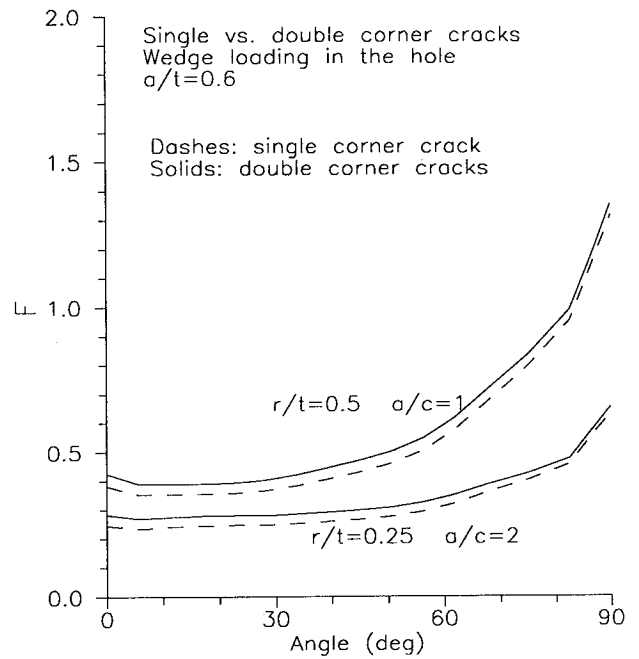


Fig. 4 (a) Comparison between single crack and double cracks.

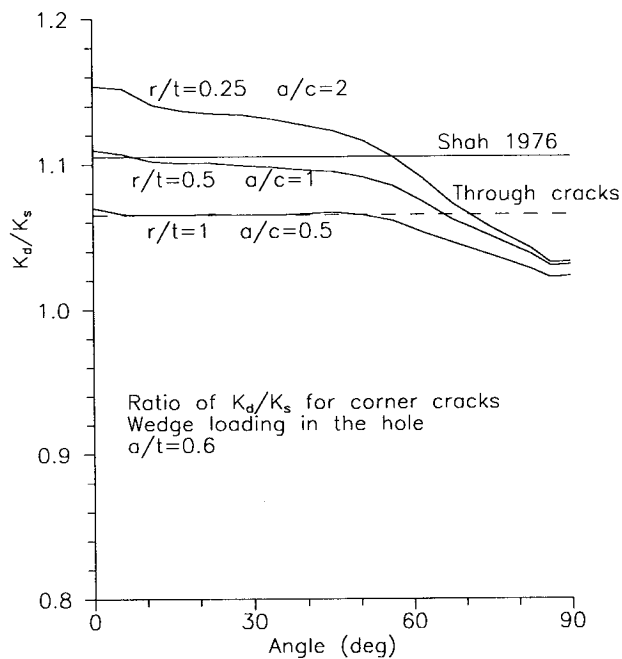


Fig. 4 (b) Ratios of stress intensity factors of double cracks to single cracks.

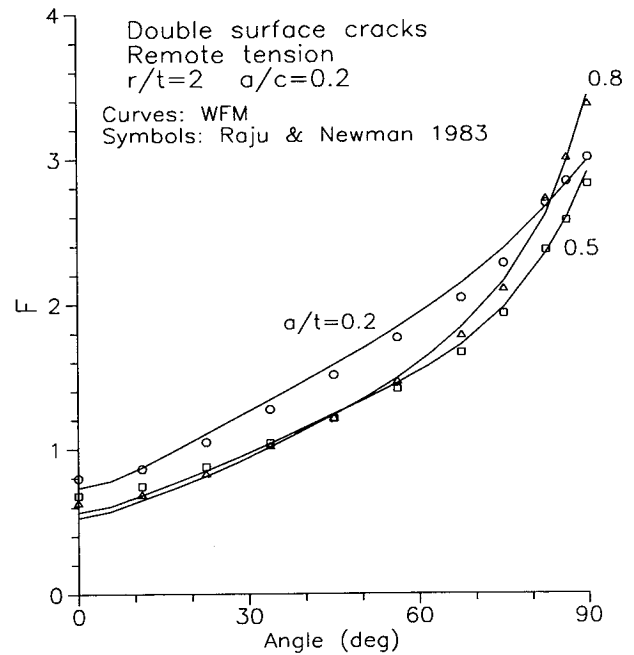


Fig. 5 Comparison with finite element solutions for surface cracks under remote tension.

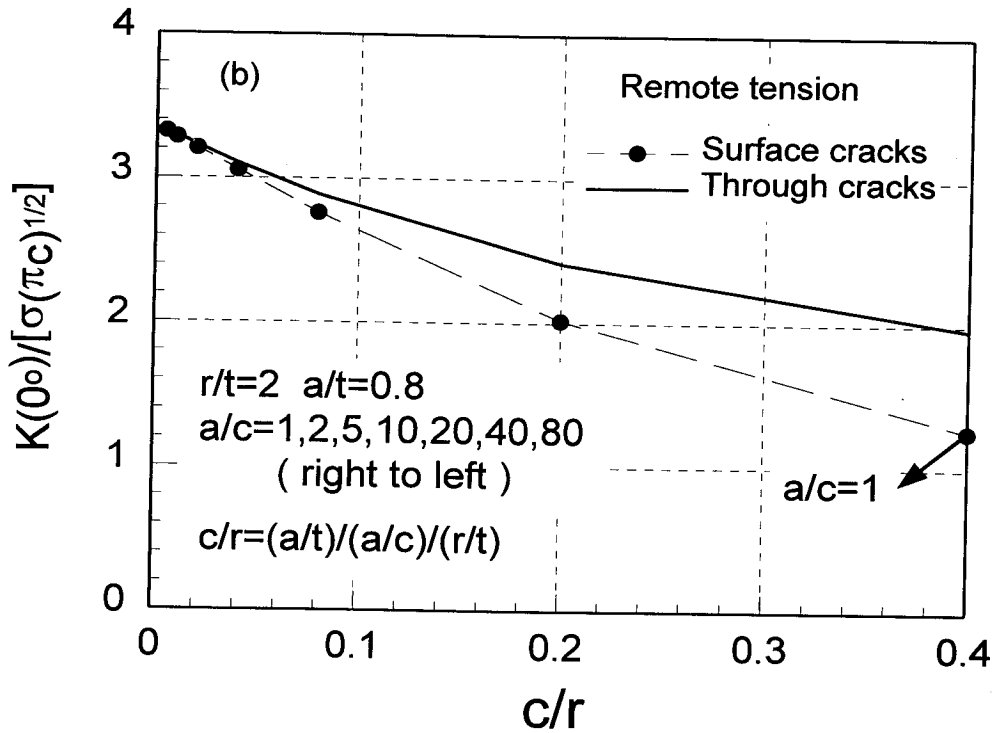
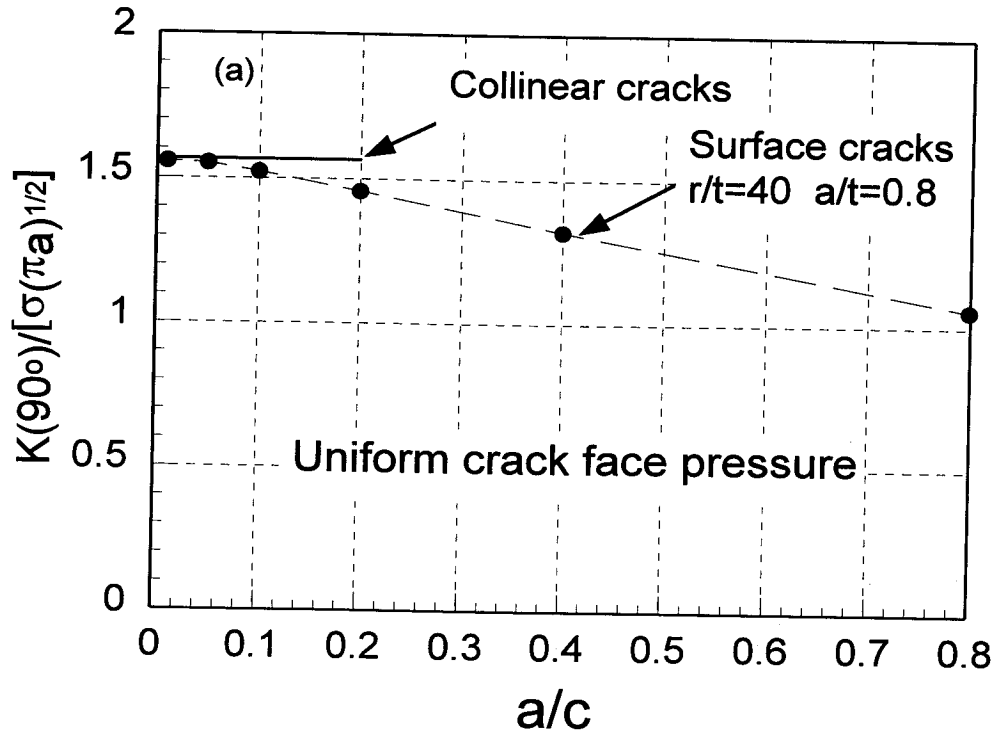


Fig. 6 Limiting behavior as (a) a/c tends to 0, (b) a/c tends to infinity.

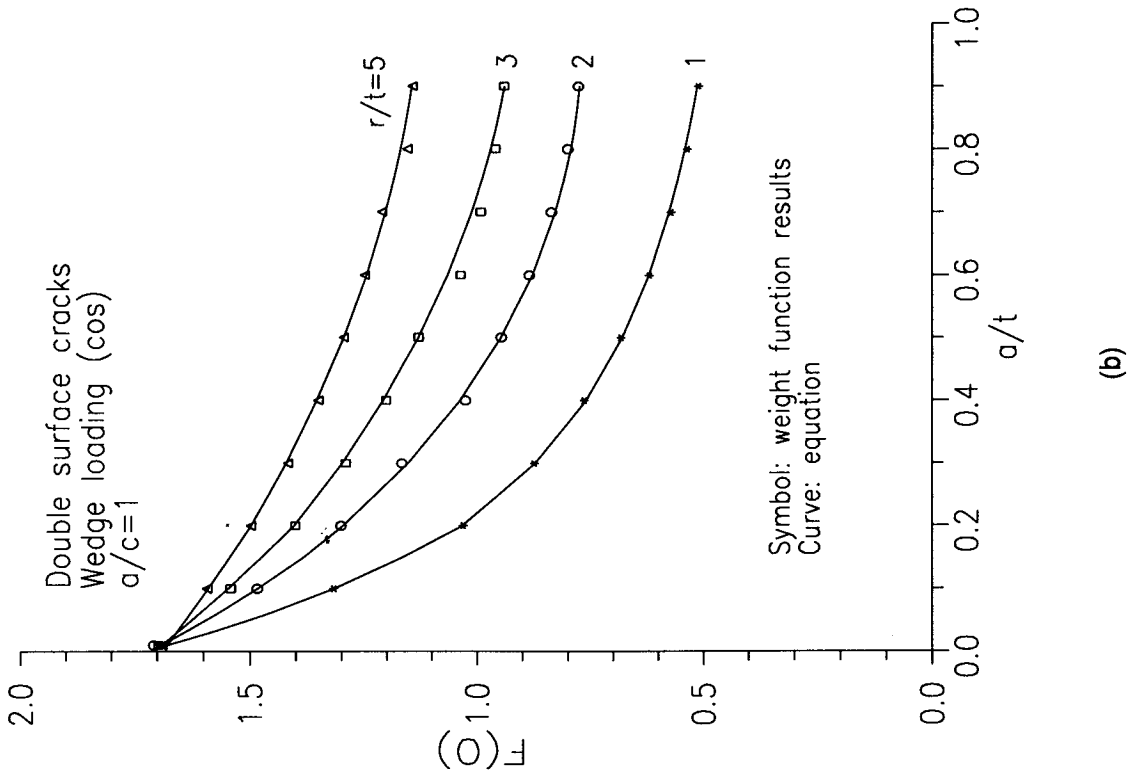
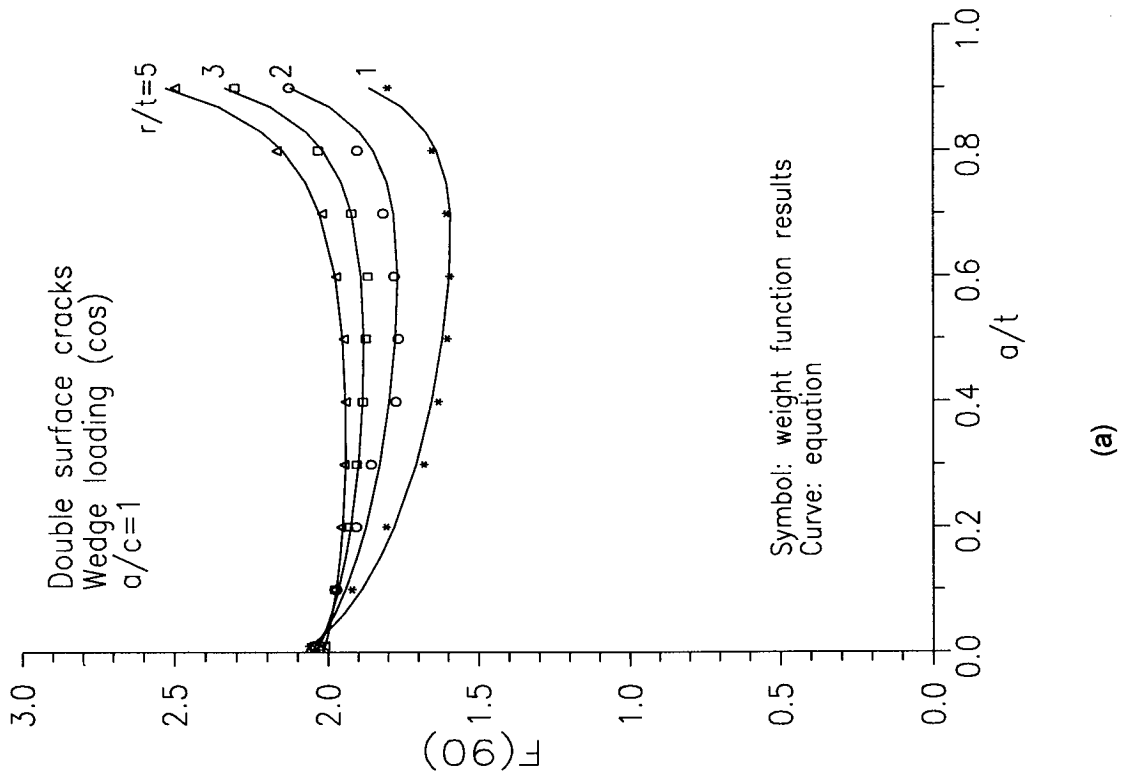


Fig. 7 Comparison of the equation with original data, (a) at 90 degree, (b) at 0 degree.

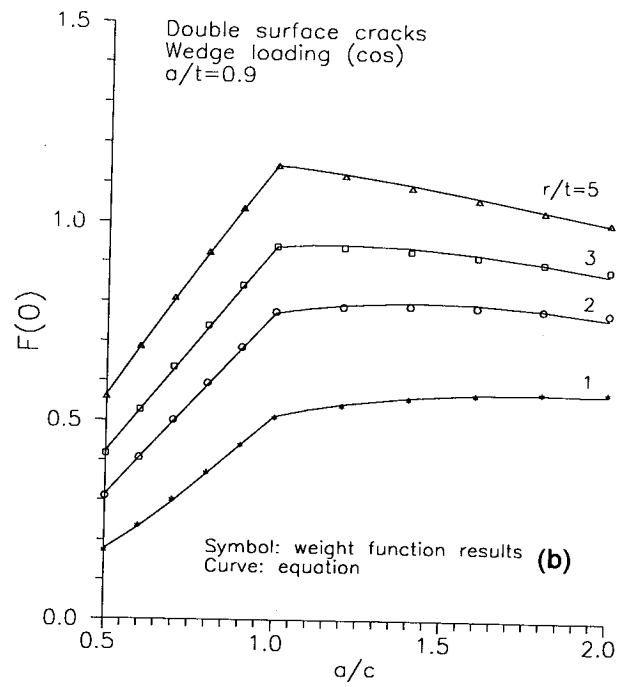
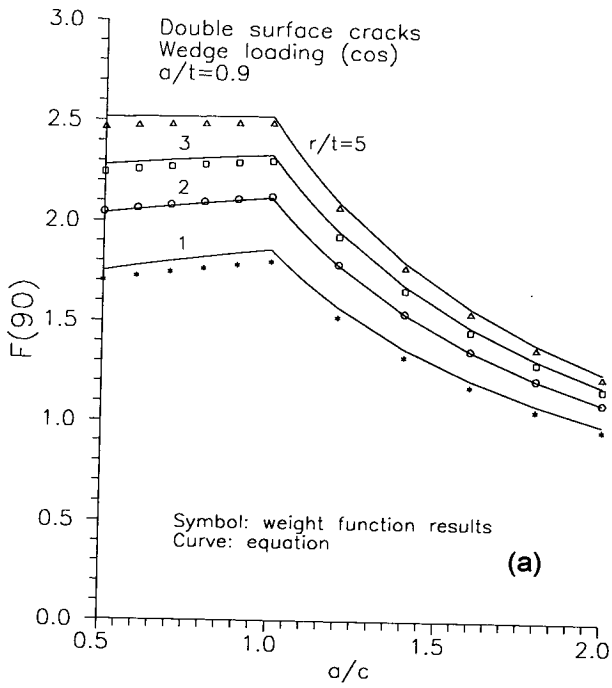


Fig. 8 Comparison of the equation with original weight function data, (a) at 90 degree, (b) at 0 degree.

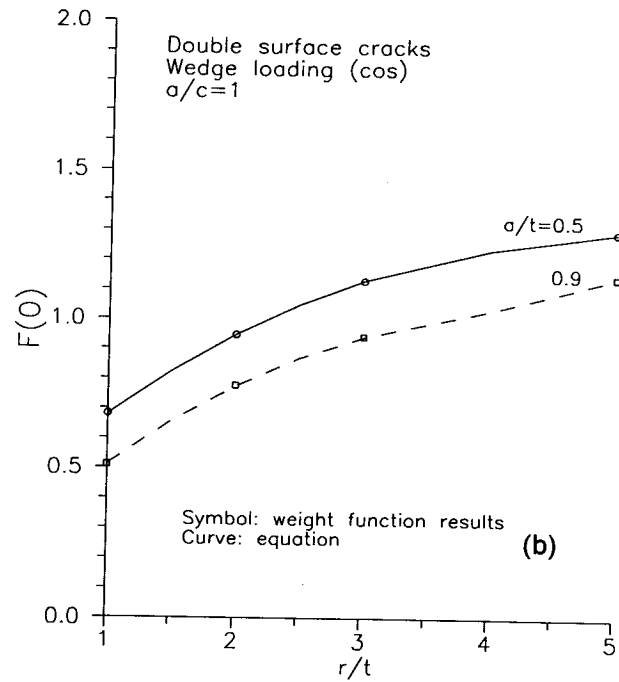
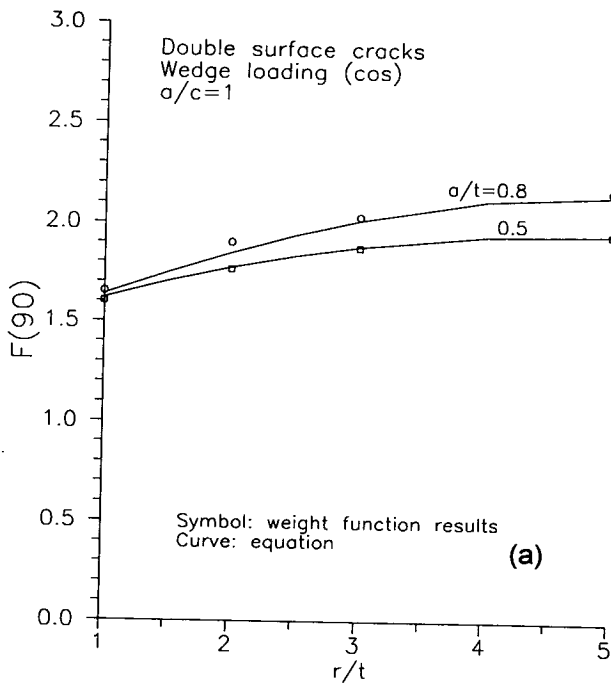


Fig. 9 Dimensionless stress intensity factor as a function of r/t ratio, (a) at 90 degree, (b) at 0 degree.